



*J. Serb. Chem. Soc.* 88 (6) 669–683 (2023)  
JSCS–5654

## Waste hemp and flax fibers and cotton and cotton/polyester yarns for removal of methylene blue from wastewater: Comparative study of adsorption properties

MARIJA M. VUKČEVIĆ<sup>1\*#</sup>, MARINA M. MALETIĆ<sup>2#</sup>, BILJANA M. PEJIĆ<sup>1</sup>, NATAŠA V. KARIĆ<sup>2#</sup>, KATARINA V. TRIVUNAC<sup>1#</sup> and ALEKSANDRA A. PERIĆ GRUJIĆ<sup>1#</sup>

<sup>1</sup>Faculty of Technology and Metallurgy, University of Belgrade, Karnegijeva 4, 11000 Belgrade, Serbia and <sup>2</sup>Innovation Center of the Faculty of Technology and Metallurgy, Karnegijeva 4, 11000 Belgrade, Serbia

(Received 13 December 2022, revised 15 March, accepted 22 March 2023)

**Abstract:** Waste hemp and flax fibers, and cotton and cotton/polyester yarns, available in large quantities from the textile industry, were used as cheap and effective sorbents for the removal of methylene blue from wastewater. Waste fibers and yarns were characterized by scanning electron microscopy, Fourier transform infrared spectroscopy, iodine sorption, water retention, and point of zero charge, as well as through the determination of crystallinity index and degree of surface crystallinity. The adsorption of methylene blue was optimized by examining the influence of contact time, initial concentration, temperature, and pH value. It was found that the more ordered structure of cotton and cotton/polyester yarns leads to lower adsorption capacities and better agreement with pseudo-second order kinetic and Langmuir isotherm model, while the more heterogeneous structure of flax and hemp fibers shows higher capacities for methylene blue adsorption, better described by the pseudo-first order kinetic and Freundlich isotherm model. Based on the obtained results, waste lignocellulosic fibers and yarns can be used for the discoloration of wastewater, thereby solving the problem of waste generated in the textile industry.

**Keywords:** textile waste; natural-based fibers; chemical composition; organic dye.

### INTRODUCTION

The high consumption of energy and non-renewable natural resources, as well as the resulting climate changes require a serious approach to sustainable environmental protection criteria, in order to ensure a decent life in modern society and preserve resources for the coming generations. Material reuse is an

\* Corresponding author. E-mail: marijab@tmf.bg.ac.rs

# Serbian Chemical Society member.

<https://doi.org/10.2298/JSC221213015V>

area of particular interest due to the large amount of waste produced around the world in various industries.<sup>1,2</sup>

The textile industry is one of the oldest and largest industries in the world, which tends to meet the ever-increasing demand for textile products that grow with the increase of the world's population.<sup>3-5</sup> Textile waste, which can be generated directly from the textile industry during the textile production processes, or post-consumer textile waste, which is created during consumer use and disposal, represents a group of reusable materials that can have different application possibilities.<sup>3,6</sup> The fact is that much more attention is paid to solving the problem of post-consumer textile waste (product reuse, material recycling, incineration and landfill)<sup>7,8</sup> than the one of the waste generated directly during textile production. Textile waste from production refers to raw textile materials, namely cellulose, protein, and synthetic fibers. Cellulose fibers are of vegetable origin, obtained from materials such as cotton, linen, hemp, ramie and straw; protein fibers are of animal origin, obtained mainly from wool, cashmere and silk, while synthetic fibers are obtained from petrochemical sources, *i.e.*, materials such as polyester, nylon, spandex, acrylic, and polypropylene.<sup>3</sup> These wastes are mainly disposed of by incineration and landfill, so, it is necessary to find ways to reuse them as materials with added value.<sup>5</sup> Another major problem in the textile industry is consuming a large amount of water used for scrolling, bleaching and dyeing processes. The textile industry is the second-largest polluter of water worldwide.<sup>9</sup> If contaminated water is not treated before discharge into natural reservoirs, this wastewater, due to its intense color, higher pH value, and high salt concentration, causes a decrease in photosynthetic activity, due to a deficiency of oxygen, which can be harmful to the aquatic ecosystem and human health.<sup>9-11</sup> According to environmental regulations, industries are required to remove dye from their wastewater before discharge into the environment. Numerous physical, chemical and biological methods may be used to remove dyes from wastewater in the textile industry. These methods mainly require specific equipment and high energy consumption, and an additional problem is the safe disposal of the removed products.<sup>11-13</sup> A process that provides low capital and energy costs, simplicity and speed, as well as high removal efficiency is adsorption.<sup>10,13</sup>

One of the effective ways to reuse textile waste is to convert them into adsorbents for wastewater treatment. Cellulose-based fibers and yarns can have exceptional adsorption properties and high absorption capacity, due to their specific structure and heterogenous chemical composition which implies the presence of different functional groups that acts as active sites for adsorption.<sup>14</sup> Summarizing all the above, it is concluded that the textile industry can be a perfect example of the reuse of textile waste material, to solve the problem of the

colored wastewater it creates. In this way, the needs for a cleaner environment and a circular economy are met at the same time.

This work examines the possibility of using waste hemp and flax fibers and cotton and cotton/polyester yarns, as cheap and effective sorbents for the removal of methylene blue from wastewater, with an emphasis on the influence that structural characteristics and chemical composition have on the adsorption properties.

#### EXPERIMENTAL

Fibers and yarns obtained as waste from different textile industries were used as adsorbents for the removal of methylene blue (MB). Short flax fibers ( $F_f$ ) were obtained from Banja Luka, Republic of Srpska, Bosnia and Herzegovina,<sup>15</sup> while hemp fibers ( $H_f$ ) were obtained from ITES Odžaci, Serbia. Waste cotton ( $C_y$ ) and cotton/polyester ( $C_y/PES$ ) yarns were obtained from SIMPO Dekor Vranje, Serbia.

Scanning electron microscopy (SEM JEOL JSM-6610LV) was used to determine the samples' morphological and structural characteristics.

The chemical composition of flax and hemp fibers and cotton yarns was determined by sequential removal of individual components from the structure of the fibers and yarns, which was in accordance with the Soutar and Bryden research.<sup>16</sup>

The surface functional groups' content was examined by Fourier transform infrared spectroscopy (Nicolet™ iS™ 10 FTIR spectrometer, ThermoFisher Scientific), in the range of 400–4000  $\text{cm}^{-1}$ . The degree of surface crystallinity ( $C_i$ ) was estimated based on the intensity of characteristic bands from the obtained FTIR spectra.<sup>17</sup> For flax and hemp fibers, and cotton yarns  $C_i$  was calculated as a ratio of the intensity of bands at 1368 and 2885  $\text{cm}^{-1}$  ( $I_{1368}/I_{2885}$ ), which were assigned to the in-the-plane C–H bending and C–H symmetrical stretching in cellulose and hemicelluloses.<sup>18</sup> Additionally, for the sample  $C_y/PES$ , the degree of surface crystallinity of the polyester component<sup>19</sup> was also calculated as the ratio between the intensity of the band at 1120  $\text{cm}^{-1}$ , related to the O–CH<sub>2</sub> stretching, and the bend at 1100  $\text{cm}^{-1}$ , related to the C–O stretching from amorphous polyester structure ( $I_{1120}/I_{1100}$ ).

Iodine sorption values ( $ISV$ ), were determined using the Schwertassek method:<sup>15</sup> yarn samples (0.3 g) were topped with iodine solution (2  $\text{cm}^3$  of  $\text{KI}_3$ ), squashed, and squeezed for 3 min. Thereafter, the saturated sodium sulfate (100  $\text{cm}^3$ ,  $w(\text{Na}_2\text{SO}_4) = 200 \text{ g dm}^{-3}$ ) was added to the yarns and shaken for 1 h. The iodine concentration of the sample and blank was determined by titration with sodium thiosulfate (0.02  $\text{mol dm}^{-3}$ ).  $ISV$  was calculated as follows:

$$ISV = \frac{(b-t) \times 2.04 \times 2.54}{m_a} \text{ mg g}^{-1} \quad (1)$$

where  $b$  and  $t$  are the volumes ( $\text{cm}^3$ ) of  $\text{Na}_2\text{S}_2\text{O}_3$  solution used for blank and sample titration, and  $m_a$  is the weight of absolute dry yarns (g).  $ISV$  was used for the determination of crystalline phase content (crystallinity index,  $X_K$ ):<sup>20</sup>

$$X_K = 100 - \left( 100 \frac{ISV}{412} \right) \quad (2)$$

The standard centrifuge method (ASTM D 2402-01 2001) was used to assess the examined samples' water retention value ( $WRV$ ).

The solid addition method<sup>21,22</sup> was used for the determination of pH at the point of zero charge ( $\text{pH}_{\text{PZC}}$ ), for all the examined samples. To a series of PP tubes, 10 ml of 0.1 M  $\text{KNO}_3$

was transferred, and the initial pH value of the solution ( $\text{pH}_i$ ) was adjusted from 2 to 10 by adding either HCl or NaOH. 0.02 g of tested fibers and yarns were added to the tubes, which were securely capped immediately. The tubes were constantly shaken for 48 h and the final pH values ( $\text{pH}_f$ ) were measured. The dependence of  $\text{pH}_f$  vs.  $\text{pH}_i$  was plotted, along with the tie line for which the final pH was considered equal to the initial pH. The intersecting point between those two lines was recognized as  $\text{pH}_{\text{pZC}}$ .

The adsorption was performed on 0.02 g of tested materials from 20 cm<sup>3</sup> MB solution (initial concentration of 20 mg dm<sup>-3</sup>), at 25 °C in the batch system for 3 h with constant shaking (170 rpm). To examine the effect of pH on adsorption, the initial pH of the MB solution was adjusted to 2, 4, 6, 8 and 10. The influence that initial concentration has on materials adsorption capacities was examined under the same conditions, using the MB solution with the initial concentration ranging from 10 to 75 mg dm<sup>-3</sup>. The influence of contact time was examined using 0.1 g of tested materials and 100 ml of MB solution (initial concentration of 20 mg dm<sup>-3</sup>), while the effect of adsorbent mass (0.01, 0.02, and 0.05 g) was studied from 20 ml of MB solution (20 mg dm<sup>-3</sup>). The concentration of MB solution was determined by UV–Vis spectrophotometry, while the amount of adsorbed MB ( $q_e$  in mg g<sup>-1</sup>) was determined as:

$$q_e = \frac{V(C_0 - C_t)}{m} \quad (3)$$

where  $C_0$  and  $C_t$  (mg L<sup>-1</sup>) are the initial concentration, and the MB concentration in the solution after a defined time, respectively;  $V$  (L) is the solution volume and  $m$  (g) is the weight of adsorbents ( $C_y$ ,  $C_y/\text{PES}$ ,  $F_f$  and  $H_f$ ).

Kinetic studies were conducted using the following kinetic models: pseudo-first-order,<sup>23</sup> and pseudo-second-order kinetic model,<sup>24</sup> Elovich<sup>25</sup> and intra-particle diffusion model,<sup>26</sup> while Langmuir<sup>27</sup> and Freundlich<sup>28</sup> isotherm models were used to interpret the equilibrium adsorption data and determine the maximum adsorption capacities of examined samples. Equations for all models used are given in Table S-I of the Supplementary material to this paper.

To evaluate the influence that surrounding temperature has on the MB adsorption, the adsorption experiments were conducted in a temperature-controlled water bath, at 25, 35 and 45 °C. The thermodynamic parameters of the adsorption process were calculated using the following equations:<sup>29</sup>

$$\ln K = \frac{\Delta S}{R} - \frac{\Delta H}{RT} \quad (4)$$

$$\Delta G = \Delta H - T\Delta S \quad (5)$$

The values of  $\Delta H$  and  $\Delta S$  were obtained from the slopes and intercepts of  $\ln K$  vs. the  $1/T$  plot, and the values of  $\Delta G$  were calculated from the corresponding values of  $\Delta H$  and  $\Delta S$  following Eq. (5).

## RESULTS AND DISCUSSION

Hemp, flax and cotton fibers are natural fibers that are characterized by complex structures, and heterogeneous chemical compositions especially distinct for hemp and flax fibers. The main structural component of these fibers is cellulose, while secondary components are hemicelluloses, lignin, pectin, fats and waxes. The content of these chemical components varies depending on the type of fiber,

as well as on geographical location, cultivation methods, and primary processing. Hemp fibers generally contain 67.0–78.3 % of cellulose, 5.5–16.1 % of hemicelluloses, 2.9–3.3 % of lignin and 0.8–2.5 % of pectin,<sup>16</sup> while flax fibers may contain 64.1–76.0 % of cellulose, 11.0–20.6 % of hemicelluloses and 2–5 % of lignin and 1.8–2.3 % of pectin.<sup>15</sup> On the other hand, cotton fibers are mainly composed of cellulose (83–99 %), and may contain some lignin (up to 6 %) and hemicelluloses and pectin (up to 5 %).<sup>30</sup>

The quantity of these constituents and their location within the fiber structure has an influence on fibers' physicochemical and mechanical properties, especially sorption properties.

The chemical composition of the examined hemp and flax fibers and cotton yarns are given in Fig. 1. It was found that cotton yarns (sample  $C_y$ , and cotton component from sample  $C_y$ /PES) contain the highest amount of cellulose (94 %) while the hemp fibers contain the highest amount of non-cellulosic components (10.7 % of hemicelluloses, and 6.06 % of lignin).

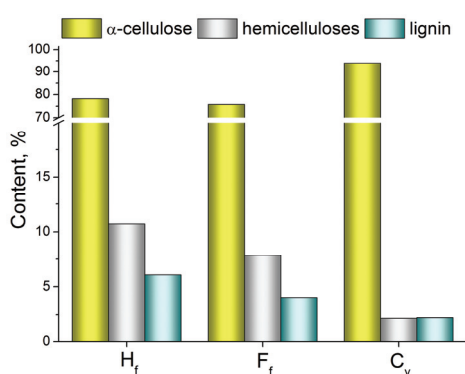


Fig. 1. Chemical composition of flax and hemp fibers and cotton yarns.

The morphology of tested fibers and yarns is examined by scanning electron microscopy (Fig. 2). The structure of flax and hemp fibers (Fig. 2a and b, respectively) is characterized by partially separated elementary fibers, which seem to be embedded in resinous substances (matrix of hemicelluloses, lignin and some pectin), and rough, uneven surface. This liberation of elementary fibers is more noticeable for flax than for hemp fibers, due to the higher content of lignin and hemicelluloses in the structure of hemp fibers. The cotton fibers within the  $C_y$  and  $C_y$ /PES structure are spirally twisted, with the structure looking like a twisted ribbon (Fig. 2c). Additionally, the polyester component from the sample  $C_y$ /PES is characterized by a straight filament, with a noticeable smooth surface.

The type, amount and availability of surface functional groups are influenced by the chemical composition and the location of the chemical components in the fiber structure. The qualitative examination of functional groups present on the surface of tested materials was performed by FTIR analysis.

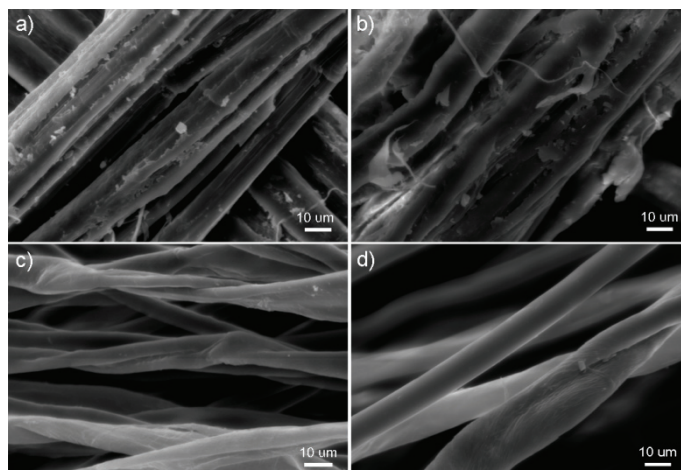


Fig. 2. SEM photographs of: a)  $H_f$ , b)  $F_f$ , c)  $C_y$  and d)  $C_y/PES$ .

FTIR spectra for all samples (Fig. 3) show a broad band around  $3300\text{ cm}^{-1}$ , originating from the stretching of the O–H bond in hydroxyl groups. Peaks at  $2850$  and  $2920\text{ cm}^{-1}$  originate from the symmetrical and asymmetrical vibrations of the C–H bond in methyl and methylene groups of cellulose and hemicelluloses<sup>31</sup> in the structure of all examined fibers and yarns. The peak near  $1730\text{ cm}^{-1}$ , attributed to C=O stretching of carbonyl or ester groups of hemicelluloses,<sup>31,32</sup> is noticeable on the spectra of samples  $F_f$  and  $H_f$ . Bands in the region  $1000\text{--}1370\text{ cm}^{-1}$ , are related to the C–O and C–C stretching in polysaccharides, cellulose, and hemicelluloses, while the peak around  $890\text{ cm}^{-1}$  indicates the presence of glucopyranose ring in the structure of all examined samples. The broad band around  $1630\text{ cm}^{-1}$ , observed for all samples, can be attributed to the aromatic skeletal vibration, or C=O stretching vibrations of hemicelluloses carbonyl groups.<sup>31</sup> Owing to the presence of polyester component, FTIR spectra of sample

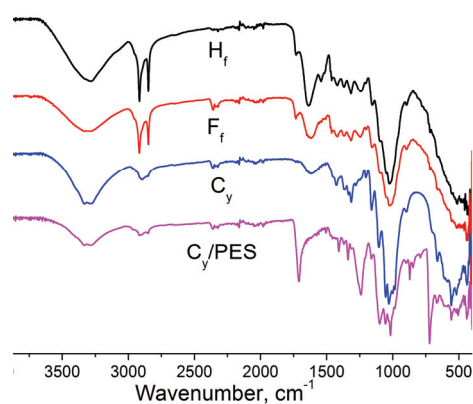


Fig. 3. FTIR spectra of flax and hemp fibers, and cotton and cotton/polyester yarns.

$C_y$ /PES showed additional, intense peaks at 1710 and 1240  $\text{cm}^{-1}$  that indicate the presence of the ester group, while the peak at 1505  $\text{cm}^{-1}$  can be attributed to the skeletal vibrations of the aromatic systems in polyester chains.<sup>33</sup> Also, out-of-plane bending vibrations of the benzene ring in the polyester are displayed at 720  $\text{cm}^{-1}$  (C–H and C=O) and 870  $\text{cm}^{-1}$  (C–C).<sup>33</sup>

The degree of surface crystallinity ( $C_i$ ), estimated based on the intensity of the characteristic bands obtained from FTIR spectra, is shown in Table I, along with the iodine sorption values ( $ISV$ ), crystallinity index ( $X_K$ ), water retention value ( $WRV$ ), and point of zero charge ( $\text{pH}_{\text{PZC}}$ ). The highest values for the degree of surface crystallinity and the crystallinity index were observed for  $C_y$ /PES, due to the presence of highly ordered polyester components and the highest content of  $\alpha$ -cellulose in the cotton component. The highly ordered structure of  $C_y$ /PES results in lower iodine adsorption, while a smooth surface (Fig. 2), observed especially for the polyester component, leads to the lowest  $WRV$ . A similar trend in the physicochemical characteristics, shown in Table I, is observed for the sample  $C_y$ , whereby  $ISV$  and  $WRV$  show higher, and  $C_i$  and  $X_K$  lower values than  $C_y$ /PES, due to the less ordered structure, which is a consequence of the absence of polyester component. Samples  $F_f$  and  $H_f$  show much higher iodine adsorption and water retention than  $C_y$  and  $C_y$ /PES samples, as well as a lower degree of surface crystallinity and crystallinity index resulting from the more heterogeneous chemical composition and the location of the components in the fiber structure. Lower content of lignin in the secondary wall, and hemicelluloses in the interfibrillar region of  $F_f$  leads to the liberation of the elementary fibers (Fig. 2) and higher availability of  $\alpha$ -cellulose on the fiber surface, making the  $F_f$  surface more crystalline than  $H_f$ . The more liberated fiber structure of  $F_f$  than  $H_f$  also results in better iodine sorption, while surface roughens and the presence of micropores and microcracks in the  $H_f$  surface leads to a higher  $WRV$ .

TABLE I. Material characterization: degree of surface crystallinity ( $C_i$ ), iodine sorption values ( $ISV$ ), crystallinity index ( $X_K$ ), water retention value ( $WRV$ ), and point of zero charge ( $\text{pH}_{\text{PZC}}$ )

Sample	$C_i$	$ISV / \text{mg I}_2 \text{ g}^{-1}$	$X_K / \%$	$WRV / \%$	$\text{pH}_{\text{PZC}}$
$H_f$	0.960	132.2	67.91	51.20	5.12
$F_f$	0.977	160.3	61.09	41.07	4.12
$C_y$	0.981	84.0	79.61	32.34	5.90
$C_y$ /PES	0.982 <sup>a</sup> 1.05 <sup>b</sup>	55.1	86.63	15.55	5.48

<sup>a</sup>Cotton component, <sup>b</sup>PES component

Adsorption characteristics of lignocellulosic fibers and yarns depend on the content of amorphous regions in cellulose and non-cellulosic components, cracks and cavities, as well as functional groups present on the absorbing surface.<sup>16,34</sup>

Accessible surface functional groups of fibers' chemical constituents (celluloses, hemicelluloses, lignin) are responsible for the surface charge and the acid–base behavior of tested samples. The  $\text{pH}_{\text{PZC}}$  values of tested samples were found to be in the range between 4.12 for  $F_f$  and 5.90 for  $C_y$  (Table I), indicating that in the water solution with pH higher than 5.90 surfaces of all tested samples will be deprotonated and negatively charged, so the adsorption of cationic MB will be favored.

The solution pH is an important factor that affects the adsorption of methylene blue through the ionization of surface functional groups along with the distribution and the morphology of dye molecules. The influence of the pH of MB solution on the adsorption capacities of examined samples is shown in Fig. 4.

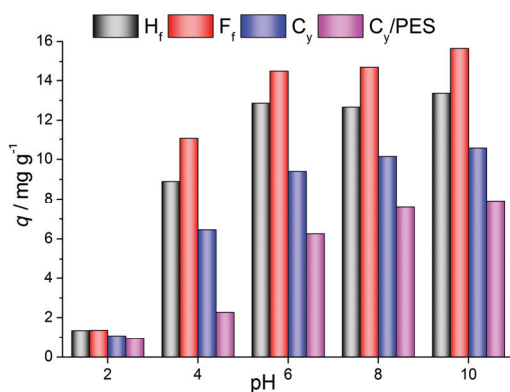


Fig. 4. Effect of the initial pH on the adsorption capacity.

Adsorption capacities increase rapidly with the increase of the solution pH from 2 to 6, while a further increase of pH slightly increases the adsorption capacities of tested samples, keeping the same trend of  $F_f > H_f > C_y > C_y/\text{PES}$ . Methylene blue is a cationic dye that is in the molecular form in the solution having a pH value lower than 4, while in the solution with a pH above 4, the  $\text{MB}^+$  becomes dominant.<sup>35</sup> Additionally, in the solution having a pH above the  $\text{pH}_{\text{PZC}}$  value, the surface of tested samples is deprotonated and negatively charged, so an increase in the pH value of the solution positively affects the attraction and bonding of  $\text{MB}^+$  species.

The influence that contact time has on the MB adsorption on tested samples is shown in Fig. 5a. Adsorption capacities follow the trend of  $F_f > H_f > C_y > C_y/\text{PES}$ , and increase with the contact time, reaching the equilibrium after 60 min of adsorption.

The process of MB removal from water solution using examined fibers and yarns is relatively fast since over 80 % of adsorption capacity was reached in the first 30 min. Experimental data were fitted with pseudo-first and pseudo-second order models (Fig. 5a), as well as with the intraparticle diffusion (Fig. 5b) and Elo-



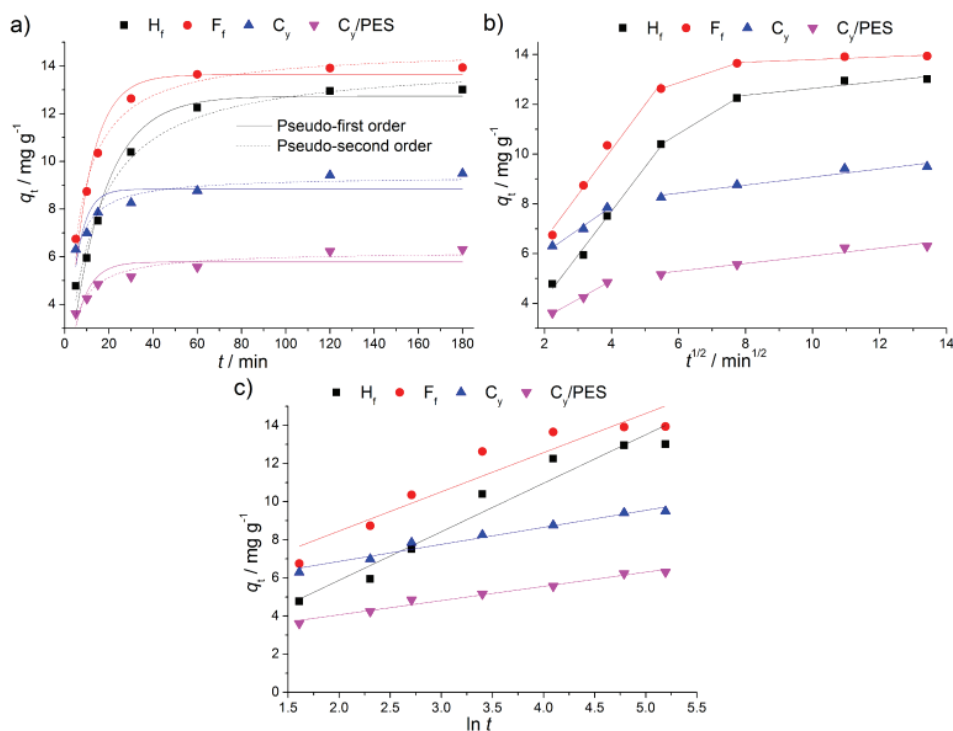


Fig. 5. Adsorption kinetic data fitted with pseudo-first and pseudo-second order (a), intraparticle diffusion (b) and Elovich (c) model.

vich (Fig. 5c) models, and the obtained kinetic parameters are given in Table S-II of the Supplementary material. According to the correlation coefficients ( $R^2$ ), adsorption of MB on all samples follow the pseudo-second order kinetic, while calculated adsorption capacity values ( $q_{e,cal}$ ) indicate that the adsorption of MB onto  $H_f$  and  $F_f$  is better described by the pseudo-first order model. The values of pseudo-first and pseudo-second rate constants indicate that the adsorption process is faster on yarns than on fiber samples. This is also noticeable from the values of Elovich constant  $\alpha$  that is related to the rate of adsorption in the beginning. Since the rate-controlling factor of the adsorption process may be the diffusion of adsorbate particles through the structure of the adsorbent, the intraparticle diffusion model was applied to the adsorption data. Multi-linear plots obtained by the intraparticle diffusion model indicate that MB adsorption onto  $H_f$  and  $F_f$  occurs through the three consecutive steps of fast external adsorption, intraparticle diffusion, and slow equilibrium adsorption, while the adsorption onto yarn samples proceeds through the external adsorption and equilibrium process. The highly ordered structure of yarn samples ( $C_i$  and  $X_K$  values), featured by smooth and nonporous cotton fibers and polyester filaments (Fig. 2), enables

only the fast adsorption onto the external surface of the yarn samples without the diffusion of the MB species into the yarn structure. Therefore, the adsorption capacities of the yarn samples are lower than for  $H_f$  and  $F_f$ , and limited by the number of active sites on the sample's external surface. The higher surface coverage of the yarn samples with MB species is confirmed by the values of Elovich constant  $\beta$ . On the other hand, higher adsorption capacities of  $F_f$  and  $H_f$  are the consequence of the more heterogeneous chemical composition and liberated fiber structure characterized by the surface roughens and the presence of micropores and microcracks.

Fig. 6 shows the influence that adsorbent mass has on the MB removal efficiency and the adsorption capacities of examined samples. For adsorbent mass 0.01 and 0.02 g removal efficiency is almost the same, while the highest removal efficiency was obtained for adsorbent mass of 0.05 g. Nevertheless, the adsorption capacities of all examined samples decrease with the increase of adsorbent mass.

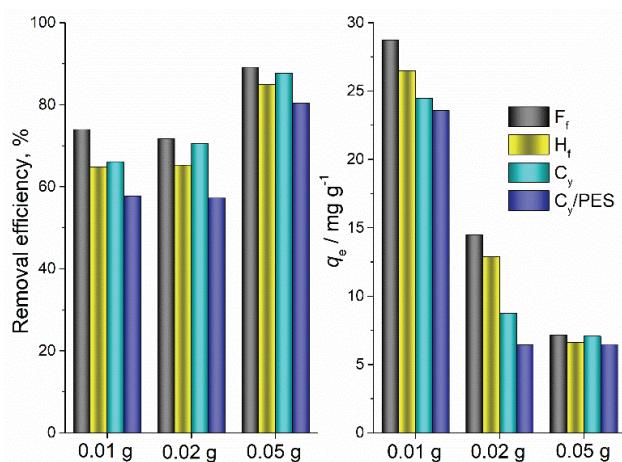


Fig. 6. The influence of adsorbent mass on MB adsorption.

The adsorption capacities of  $F_f$  and  $H_f$  increase with the initial concentration of MB solution (Fig. 7), while for samples  $C_y$  and  $C_y/PES$ , an increase in a concentration above 30 and 20 mg dm<sup>-3</sup>, respectively, does not increase adsorption capacities, due to the surface saturation.

The obtained values for Langmuir and Freundlich parameters (Table II) are in agreement with the sample structure's influence on MB adsorption. The more amorphous and porous structure of  $H_f$  and  $F_f$  samples leads to higher maximal adsorption capacities ( $Q_0$ ) and surface heterogeneity ( $1/n$ ), whereby the Freundlich isotherm better describes the adsorption of MB on these samples. Samples

$C_y$  and  $C_y$ /PES show lower adsorption capacities, more homogeneous surfaces, and better fits with Langmuir isotherm.

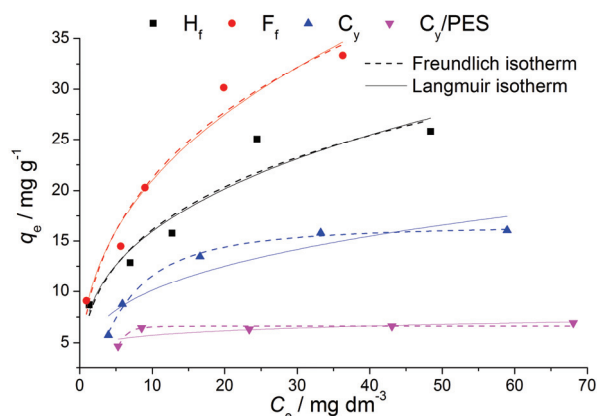


Fig. 7. The influence of initial concentration on MB adsorption: equilibrium adsorption data fitted with Langmuir and Freundlich isotherm.

TABLE II. Langmuir and Freundlich isotherm parameters for MB adsorption on examined fibers and yarns samples.

Sample	Langmuir isotherm			Freundlich isotherm		
	$Q_0 / \text{mg g}^{-1}$	$b$	$R^2$	$K_f / \text{mg}^{1-1/n} \text{L}^{1/n} \text{g}^{-1}$	$1/n$	$R^2$
$H_f$	104.063	0.0713	0.84306	7.350	0.337	0.89365
$F_f$	142.625	0.0601	0.92953	8.569	0.389	0.95157
$C_y$	16.630	0.0712	0.99077	4.987	0.307	0.84602
$C_y$ /PES	6.618	0.000169	0.88299	4.502	0.105	0.50585

Thermodynamic studies revealed that MB adsorption onto tested fibers and yarns is an exothermic process (Table III) and that an increase in surrounding temperature leads to a decrease in the adsorption capacities (Fig. S-1 of the Supplementary material). The increase in temperature leads to higher MB solubility and a decrease in the attraction forces between the MB particles and the adsorbent surface.<sup>36</sup> The adsorption process is spontaneous for  $H_f$  and  $F_f$  at all tested temperatures, and for  $C_y$  at 25 and 35 °C, while the adsorption on  $C_y$ /PES is not spontaneous.

#### CONCLUSION

The conducted investigation was focused on reusing short and entangled flax and hemp fibers, and cotton and cotton/polyester yarns, obtained as waste from the textile industry, as a sustainable and renewable adsorbent for the purification of textile industry wastewaters. The adsorption properties of examined lignocellulosic fibers and yarns depend on chemical composition and the location of the structural constituents within the fiber structure. The higher content of  $\alpha$ -cellulose and

TABLE III. Thermodynamic parameters for MB adsorption onto examined fibers and yarns

Sample	$T / \text{K}$	$q_e / \text{mg g}^{-1}$	Thermodynamic parameters		
			$\Delta G / \text{kJ mol}^{-1}$	$\Delta H / \text{kJ mol}^{-1}$	$\Delta S / \text{kJ mol}^{-1} \text{K}^{-1}$
$H_f$	298.15	15.20	-2.95	-21.994	-0.064
	308.15	14.47	-2.31		
	318.15	12.88	-1.67		
$F_f$	298.15	13.95	-2.19	-24.443	-0.075
	308.15	13.28	-1.45		
	318.15	10.40	-0.70		
$C_v$	298.15	11.01	-0.72	-17.931	-0.058
	308.15	10.23	-0.14		
	318.15	8.90	0.44		
$C_v/\text{PES}$	298.15	8.09	0.84	-16.893	-0.059
	308.15	7.31	1.44		
	318.15	6.10	2.03		

the presence of polyester component led to the lower adsorption capacities of cotton and cotton/polyester yarns, while the adsorption process follows the pseudo-second order kinetic and can be described by Langmuir isotherm. On the other hand, more heterogeneous chemical composition and presence of non-cellulosic components in the structure of flax and hemp fibers, as well as fibrillated structure and presence of cavities and cracks on the fiber surface led to the higher capacities for removal of MB from water. The MB adsorption onto the heterogeneous surface of hemp and flax fibers is well described by the pseudo-first order kinetic model and Freundlich isotherm, whereby the intraparticle diffusion affects the rate of adsorption. Based on the obtained results, waste lingo-cellulosic fibers and yarns can be applied for the discoloration of wastewater, thereby solving the problem of wastes generated in the textile industry.

#### SUPPLEMENTARY MATERIAL

Additional data and information are available electronically at the pages of journal website: <https://www.shd-pub.org.rs/index.php/JSCS/article/view/12170>, or from the corresponding author on request.

*Acknowledgement.* This research was supported by the Science Fund of the Republic of Serbia, GRANT No 7743343, Serbian Industrial Waste towards Sustainable Environment: Resource of Strategic Elements and Removal Agent for Pollutants – SIW4SE, Program IDEAS.

## ИЗВОД

ОТПАДНА ВЛАКНА КОНОПЉЕ И ЛАНА И ПРЕЂЕ ПАМУКА И ПАМУК/ПОЛИЕСТЕРА  
ЗА УКЛАЊАЊЕ МЕТИЛЕНСКО ПЛАВОГ ИЗ ОТПАДНЕ ВОДЕ: УПОРЕДНА АНАЛИЗА  
АДСОРПЦИОНИХ КАРАКТЕРИСТИКА

МАРИЈА М. ВУКЧЕВИЋ<sup>1</sup>, МАРИНА М. МАЛЕТИЋ<sup>2</sup>, БИЉАНА М. ПЕЈИЋ<sup>1</sup>, НАТАША В. КАРИЋ<sup>2</sup>,  
КАТАРИНА В. ТРИВУНАЦ<sup>1</sup> и АЛЕКСАНДРА А. ПЕРИЋ ГРУЈИЋ<sup>2</sup>

<sup>1</sup>Технолошко–механички факултет, Универзитета у Београду, Карнегијева 4, 11000 Београд, и

<sup>2</sup>Иновациони центар Технолошко–механичког факултета, Карнегијева 4, 11000 Београд

Отпадна влакна конопље и лана и пређе памука и памук/полиестра, добијена као отпад из текстилне индустрије, коришћена су као јефтине и ефикасне сорбенти за уклањање метиленског плавог из отпадних вода. Узорци влакана и пређе су окарактерисани скенирајућом електронском микроскопијом, инфрацрвеном спектроскопијом са Фуријеовом трансформацијом, сорпцијом јода, задржавањем воде, тачком нултог наелектрисања, као и одређивањем индекса кристаличности и степена површинске кристаличности. У циљу оптимизације адсорпције метиленско плавог испитан је утицај времена контакта, почетне концентрације, температуре и рН вредности на ефикасност адсорпције. Показано је да пређа памука и памук/полиестра са већим уделом кристалних области у структури има нижи адсорпциони капацитет и боље се слаже са кинетичким моделом псеудо-другог реда и Лангмировом адсорпционом изотермом. С друге стране, влакна лана и конопље се одликују већим уделом аморфних области и нецелулозних компоненти у структури и показују већи капацитет адсорпције и боље слагање са кинетичким моделом псеудо-првог реда као и са Фројндлиховом адсорпционом изотермом. На основу добијених резултата показано је да се отпадна лигноцелулозна влакна и пређа могу користити за обезбојавање отпадних вода, чиме се решава проблем отпада који настаје у текстилној индустрији и задовољавају све строжији захтеви у области заштите животне средине.

(Примљено 13. децембра 2022, ревидирано 15. марта, прихваћено 22. марта 2023)

## REFERENCES

1. A. Briga-Sá, D. Nascimento, N. Teixeira, J. Pinto, F. Caldeira, H. Varum, A. Paiva, *Constr. Build. Mater.* **38** (2013) 155 (<https://doi.org/10.1016/j.conbuildmat.2012.08.037>)
2. Y. Wang, *Waste Biomass Valor.* **1** (2010) 135 (<http://dx.doi.org/doi:10.1007/s12649-009-9005-y>)
3. N. Pensupa, S.Y. Leu, Y. Hu, C. Du, H. Liu, H. Jing, H. Wang, C.S. Ki Lin, *Top. Curr. Chem.* **375** (2017) 189 (<http://dx.doi.org/doi:10.1007/s41061-017-0165-0>)
4. Yalcin-Enis, M. Kucukali-Ozturk, H. Sezgin, in *Nanoscience and Biotechnology for Environmental Applications*, K.M. Gothandam, S. Ranjan, N. Dasgupta, E. Lichtfouse, Eds., Springer Nature Switzerland AG, Cham, 2019, p. 29 ([http://dx.doi.org/doi:10.1007/978-3-319-97922-9\\_2](http://dx.doi.org/doi:10.1007/978-3-319-97922-9_2))
5. J. Rapsikevičienė, I. Gorauskienė, A. Jučienė, *Environ. Res. Eng. Manage.* **75** (2019) 43 (<http://dx.doi.org/doi:10.5755/j01.ere.m.75.1.21703>)
6. S. Rizal, K.H.P.S. Abdul, A.A. Oyekanmi, O.N. Gideon, C.K. Abdullah, E.B. Yahya, T. Alfatah, F.A. Sabaruddin, A.A. Rahman, *Polymers* **13** (2021) 1 (<http://dx.doi.org/doi:10.3390/polym13071006>)
7. D. Tian, Z. Xu, D. Zhang, W. Chen, J. Cai, H. Deng, Z. Sun, Y. Zhou, *J. Solid State Chem.* **269** (2018) 580 (<http://dx.doi.org/doi:10.1016/j.jssc.2018.10.035>)

8. M.D. Stanescu, *Environ. Sci. Pollut. Res.* **28** (2021) 14253 (<http://dx.doi.org/doi:10.1007/s11356-021-12416-9>)
9. F. Parvin, S. Islam, Z. Urmy, S. Ahmed, A.K.M. Saiful Islam, *Biomed. J. Sci. Technol. Res.* **28** (2020) 21831 (<http://dx.doi.org/doi:10.26717/BJSTR.2020.28.004692>)
10. S. Mor, M.K. Chhavi, K.K. Sushil, K. Ravindra, *Environ. Dev. Sustain.* **20** (2018) 625 (<http://dx.doi.org/doi:10.1007/s10668-016-9902-8>)
11. M.D. Tenev, A. Fariás, C. Torre, G. Fontana, N. Caracciolo, S.P. Boeykens, *J. Sustain. Develop. Energy, Water Environ. Systems* **7** (2019) 667 (<http://dx.doi.org/doi:10.13044/j.sdewes.d7.0269>)
12. S. Khamparia, D. Kaur Jaspal, *Front. Env. Sci. Eng.* **11** (2017) 1 (<http://dx.doi.org/doi:10.1007/s11783-017-0899-5>)
13. S. Rangabhashiyam, N. Anu, N. Selvaraju, *J. Environ. Chem. Eng.* **1** (2013) 629 (<http://dx.doi.org/doi:10.1016/j.jece.2013.07.014>)
14. M. Kostic, B. Pejic, M. Vukcevic, in *Chemistry of Lignocellulosics: Current Trends*, T. Stevanovic, Ed., Taylor & Francis Group/CRC Press, Boca Raton, FL, 2018, p. 3 (<https://www.crcpress.com/Chemistry-of-Lignocellulosics-Current-Trends/Stevanovic/p/book/9781498775694>)
15. B.D. Lazić, B.M. Pejić, A.D. Kramar, M.M. Vukčević, K.R. Mihajlovski, J.D. Rusmirović, M.M. Kostić, *Cellulose* **25** (2018) 697 (<https://doi.org/10.1007/s10570-017-1575-4>)
16. Pejić, M. Vukčević, M. Kostić, in *Sustainable Agriculture Reviews 42*, G. Crini, E. Lichtfouse, Eds., Springer Nature Switzerland AG, Cham, 2020, p. 111 ([https://doi.org/10.1007/978-3-030-41384-2\\_4](https://doi.org/10.1007/978-3-030-41384-2_4))
17. J.G.G. De Farias, R.C. Cavalcante, B.R. Canabarro, H.M. Viana, S. Scholz, R.A. Simão, *Carbohydr. Polym.* **165** (2017) 429 (<http://dx.doi.org/10.1016/j.carbpol.2017.02.042>)
18. Dai, M. Fan, *Vib. Spectrosc.* **55** (2011) 300 (<http://dx.doi.org/10.1016/j.vibspec.2010.12.009>)
19. Donelli, G. Freddi, V.A. Nierstrasz, Paola Taddei, *Polym. Degrad. Stabil.* **95** (2010) 1542 (<http://dx.doi.org/10.1016/j.polymdegradstab.2010.06.011>)
20. Fakin, V. Golob, K. Stana Kleinschek, A. Majcen, L. Marechal, *Text. Res. J.* **76** (2006) 448 (<http://dx.doi.org/10.1177/0040517506062767>)
21. M. Vukcevic, B. Pejic, M. Lausevic, I. Pajic-Lijakovic, M. Kostic, *Fiber. Polym.* **15** (2014) 687 (<http://dx.doi.org/10.1007/s12221-014-0687-9>)
22. N. Saha, M. Volpe, L. Fiori, R. Volpe, A. Messineo, M. Toufiq Reza, *Energies* **13** (2020) 4686 (<http://dx.doi.org/10.3390/en13184686>)
23. S. Lagergren, *Handlingar* **24** (1898) 1
24. Y. S. Ho, G. Mckay, *Process Biochem.* **34** (1999) 451 ([http://dx.doi.org/10.1016/S0032-9592\(98\)00112-5](http://dx.doi.org/10.1016/S0032-9592(98)00112-5))
25. W.J. Weber, J.C. Morris, *J. Sanit. Eng. Div. Am. Soc. Civil. Eng.* **89** (1963) 31
26. C. Aharoni, M. Ungarish, *J. Chem. Soc. Faraday Trans. 1* (1976) 265 (<https://doi.org/10.1039/F19767200400>)
27. Langmuir, *J. Am. Chem. Soc.* **40** (1918) 1361
28. H.M.F. Freundlich, *Phys. Chem.* **57** (1906) 384
29. Harrou, E. Gharibi, H. Nasri, M. El Ouahabi, *SN Appl. Sci.* **2** (2020) 277 (<https://doi.org/10.1007/s42452-020-2067-y>)
30. R.M. Kozasowski, M. Mackiewicz-Talarczyk, A.M. Allam, in *Handbook of Natural Fibres Volume 1*, R.M. Kozłowski, Ed., Woodhead Publishing Limited, Sawston, Cambridge, 2012, p. 56

31. H. Zhang, R. Ming, G. Yang, Y. Li, Q. Li, H. Shao, *Polym. Eng. Sci.* **55** (2015) 2553 (<https://doi.org/10.1002/pen.24147>)
32. M.A. Sawpan, K.L. Pickering, Alan Fernyhough, *Compos., A* **42** (2011) 888 (<https://doi.org/10.1016/j.compositesa.2011.03.008>)
33. A.A. Younis, *Egypt. J. Pet.* **25** (2016) 161 (<http://dx.doi.org/10.1016/j.ejpe.2015.04.001>)
34. S. Mihajlović, M. Vukčević, B. Pejić, A. Perić-Grujić, M. Ristić, K. Trivunac, *J. Nat. Fibers* (2021) 9860 (<https://doi.org/10.1080/15440478.2021.1993414>)
35. J.J. Salazar-Rabago, R. Leyva-Ramos, J. Rivera-Utrilla, R. Ocampo-Perez, F.J. Cerino-Cordova, *Sustain. Environ. Res.* **27** (2017) 32 (<http://dx.doi.org/10.1016/j.serj.2016.11.009>)
36. Salah Omer, G.A. El Naeem, A.I. Abd-Elhamid, O.O.M. Farahat, A.A. El-Bardan, He.M.A. Soliman, A.A. Nayl, *J. Mater. Res. Technol.* **19** (2022) 3241 (<https://doi.org/10.1016/j.jmrt.2022.06.045>).